



Original article

The Substrate-Activity-Screening methodology applied to receptor tyrosine kinases: A proof-of-concept study

Julien Chapelat^a, Frédéric Berst^{a,*}, Andreas L. Marzinzik^a, Henrik Moebitz^a, Peter Drueckes^a, Joerg Trappe^a, Doriano Fabbro^a, Dieter Seebach^b^a Novartis Institutes for BioMedical Research, Novartis Campus, CH-4002 Basel, Switzerland^b Eidgenössische Technische Hochschule, CH-8092 Zurich, Switzerland

ARTICLE INFO

Article history:

Received 2 May 2012

Received in revised form

22 July 2012

Accepted 26 August 2012

Available online 4 September 2012

Keywords:

Kinase inhibitor

Substrate-Activity-Screening

Protein–protein interactions

Michaelis–Menten kinetics

Insulin-like Growth Factor 1 Receptor

ABSTRACT

Protein kinases are widely recognized as important therapeutic targets due to their involvement in signal transduction pathways. These pathways are tightly controlled and regulated, notably by the ability of kinases to selectively phosphorylate a defined set of substrates. A wide variety of disorders can arise as a consequence of abnormal kinase-mediated phosphorylation and numerous kinase inhibitors have earned their place as key components of the modern pharmacopeia. Although “traditional” kinase inhibitors typically act by preventing the interaction between the kinase and ATP, thus stopping substrate phosphorylation, an alternative approach consists in disrupting the protein–protein interaction between the kinase and its downstream partners. In order to facilitate the identification of potential chemical starting points for substrate-site inhibition approaches, we desired to investigate the application of Substrate Activity Screening to kinases. We herein report a proof-of-concept study demonstrating, on a model tyrosine kinase, that the key requirements of this methodology can be met. Namely, using peptides as model substrates, we show that a simple ADP-accumulation assay can be used to monitor substrate efficiency and that efficiency can be optimized in a modular manner. More importantly, we demonstrate that structure–efficiency relationships translate into structure–activity relationships upon conversion of the substrates into inhibitors.

© 2012 Elsevier Masson SAS. All rights reserved.

1. Introduction and design

The role of protein kinases in signal transduction pathways has been extensively studied over the past years, revealing their ability to switch various cellular processes on or off. As a consequence of abnormal kinase-mediated phosphorylation, many diseases arise such as cancer, diabetes, rheumatoid arthritis and hypertension [1]. This diversity of therapeutic indications has elevated kinases to the rank of high priority targets for the pharmaceutical industry. Although most of the efforts in the development of inhibitors concern ATP mimetic compounds [2], many disadvantages have been identified such as kinome selectivity, competing against high concentrations of ATP in cells and an increasingly congested intellectual property landscape. As a consequence, alternative approaches for kinase inhibition have been envisaged such as the elaboration of potent and selective non-ATP site-directed ligands able to alter kinase function [3]. Disrupting the interactions

between the kinase and its peptidic substrates represents another attractive paradigm to modulate kinase function and several substrate-site ligands have been reported over the last decade [4]. However, a significant hurdle hampering the identification of kinase-substrate protein–protein interaction inhibitors often lies in characterizing the binding site and ruling out other allosteric actions on either the kinase or its substrate [5].

In 2007, Ellman et al. reported a novel approach for the identification of substrate-targeted phosphatase inhibitors – the Substrate Activity Screening (SAS) methodology – that relied on the identification and optimization of PtpB substrates that were subsequently turned into inhibitors through replacement of the reactive phosphate by an inert isostere (Fig. 1) [6]. We envisaged that the application of this strategy to kinases would have significant advantages over the common inhibitor screening methodologies. Indeed, substrate-site inhibitor starting points are generally weak, which imposes technical limitations on their detection (displacement of a weak reference substrate required for detection and lack of dynamic range). In addition, inhibitor screening typically provides no information on mode-of-action and additional studies must be carried out to rule out inadvertent competition

* Corresponding author. Tel.: +41 (0)61 324 6011; fax: +41 (0)61 324 8001.

E-mail address: frederic.berst@novartis.com (F. Berst).

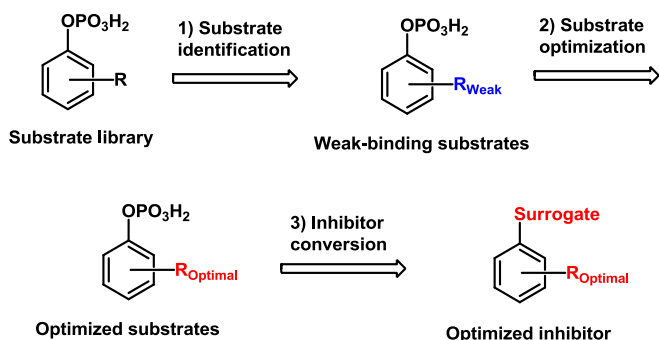


Fig. 1. Identification of PtpB substrate-targeted inhibitor by the SAS methodology.

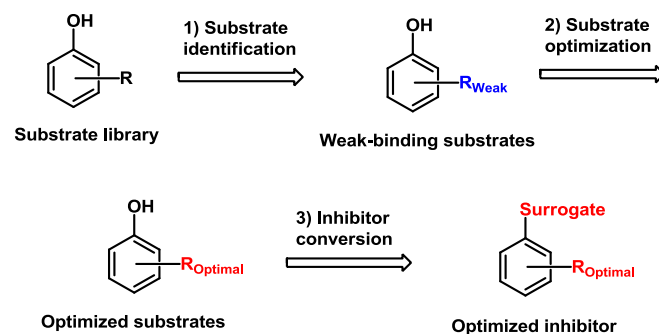


Fig. 2. General strategy for the identification of substrate-targeted tyrosine kinase inhibitors.

with ATP, interaction with the competition substrate or an allosteric mechanism. Conversely, detection of substrate phosphorylation is a direct, mechanistic readout ensuring that the recognition event happens in the substrate site. Furthermore, assays can be designed that amplify the signal resulting from even minute amounts of phosphorylation, thus facilitating the establishment of structure–activity relationships (SAR).

As part of a larger program aiming at identifying non-ATP site-directed inhibitors of tyrosine kinases, we envisaged to adapt the SAS methodology to this class of receptors and obtain a proof of concept. The methodology can be summarized in three steps (Fig. 2): (Step 1) a diverse, modular initial library of phenols is synthesized by decoration of suitable low molecular weight scaffolds. The library is then screened for phosphorylation by the tyrosine kinase of interest, (Step 2) phenolic hits are optimized in a multidimensional fashion to increase their substrate efficiency (the phenol is retained as the assay readout depends on its presence) and (Step 3) finally, the phenolic moiety is removed and the substrate is thereby turned into an inhibitor.

In order to obtain a proof of concept, it must be shown that: (a) an assay with sufficient dynamic range can be identified to detect minute amounts of phosphorylation, (b) substrate phosphorylation can be optimized in a modular fashion, (c) a correlation can be established, under certain conditions, between the phosphorylation efficiency of the substrate (K_M , substrate) and its ability to bind to the kinase (K_D , substrate) and (d) the binding SAR observed for the substrate can be transferred to the corresponding inhibitors (K_D , inhibitor). It is important to note that this methodology has the ambition to provide a suitable starting point for further medicinal chemistry optimization and does not claim to be a comprehensive screening method. Indeed, the scaffold decoration approach inherently biases chemical matter. Moreover, poor substrates but otherwise suitable ligands, in other words competent inhibitors, would not be identified by the methodology. We did not foresee this to be an issue, since kinase inhibition assays are typically part of the usual arsenal of a kinase medicinal chemistry program and

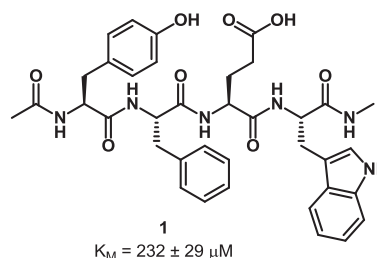


Fig. 3. Tetrapeptide **1** identified from IGF-1R substrate profiling [7].

the discovery phenol library can easily be added to routine screening campaigns. Poor dissociation of the phosphorylated product from the kinase (product inhibition) was perceived as another potential source of false negatives, albeit mitigated by the fact that phosphorylated substrates usually rapidly dissociate from the protein, thus ensuring that the binding site is free for the next substrate molecule.

2. Results and discussion

To set the stage for our study, we required a well-characterized kinase–substrate pair as well as an enzymatic assay with a suitable dynamic range. We therefore decided to make use of previous work carried out in our laboratory, which led to the identification of an efficient tetrapeptide substrate **1** of Insulin-like Growth Factor 1 Receptor (IGF-1R) (Fig. 3) [7]. This allowed us to circumvent the costly synthesis of a diverse, modular low-molecular-weight phenol library to provide the initial substrate hit from “step 1”. Moreover, we had already shown that the kinetic enzymatic assay (ADP Quest™ [8]) used to profile the substrate specificity of IGF-1R enabled the determination of K_M constants down to 2.5 μM while still satisfying the Michaelis–Menten assumptions [9], thus making it an ideal tool for our purpose.

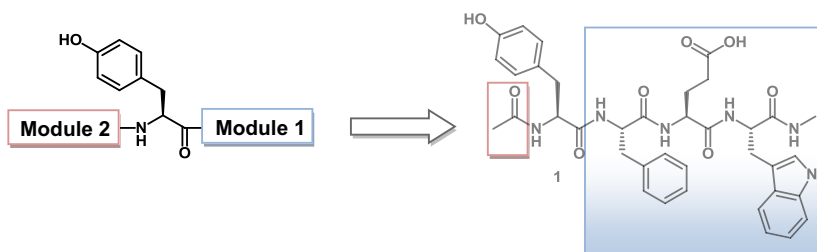
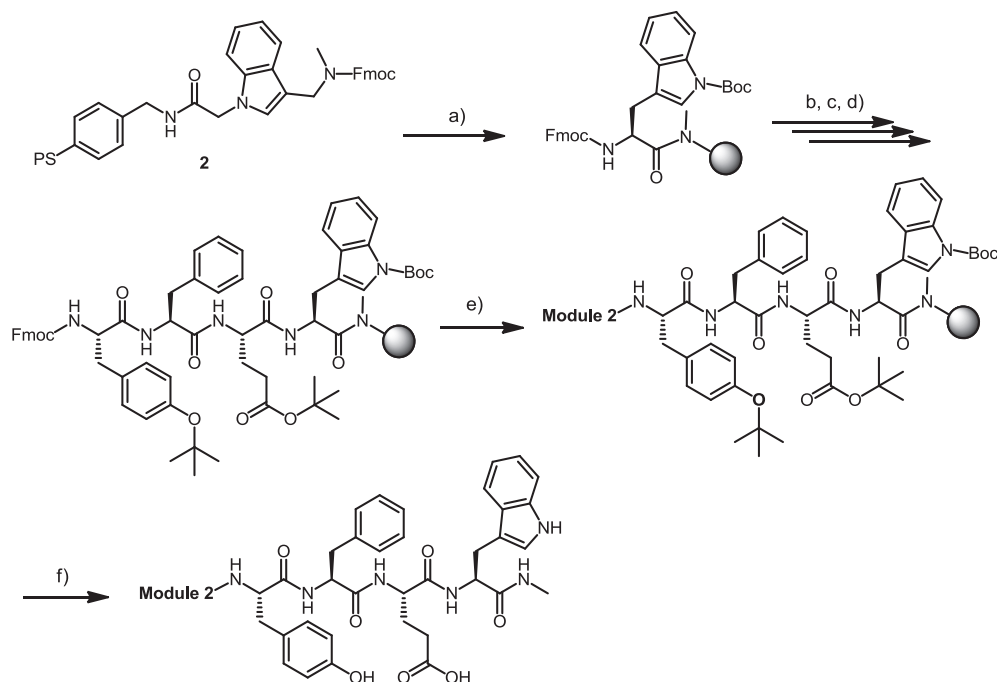


Fig. 4. Modified optimization strategy: using tetramer **1** as initial hit.



Scheme 1. Solid phase synthesis of the M2-library of substrates. a) DMA:Piperidine (4:1), 3×30 min then Fmoc-Trp(Boc)-OH, HCTU, DIEA, NMP, 2×90 min; b) DMA:Piperidine (4:1), 3×30 min then Fmoc-Glu(tBu)-OH, HCTU, DIEA, NMP, 90 min; c) DMA:Piperidine (4:1), 3×30 min then Fmoc-Phe-OH, HCTU, DIEA, NMP, 90 min; d) DMA:Piperidine (4:1), 3×30 min then Fmoc-Tyr(tBu)-OH, HCTU, DIEA, NMP, 90 min; e) DMA:Piperidine (4:1), 3×30 min then Module 2-COOH, HCTU, DIEA, NMP, 90 min; f) TFA:TIS:H₂O (95:2.5:2.5), 3×30 min.

According to our proposal, the tetrapeptide **1** was formally decomposed into a phenol-containing scaffold (tyrosine) flanked by two diversity elements: module 1 (M1: FEW-NHMe) and module 2 (M2: acetyl, Fig. 4). We set out to demonstrate that M1 and M2 could be optimized independently and that the combination of optimal moieties would lead to the most efficient substrate. The next logical step to obtain final proof-of-concept would be to

confirm the transfer of substrate SAR to inhibitor SAR upon replacement of the phenol moiety.

We therefore synthesized a first library incorporating 125 structurally diverse carboxylic acid modules 2 by Fmoc/tBu-Boc solid-phase peptide synthesis on a Prelude peptide synthesizer (Protein Technologies Inc.). The indole-functionalized acid-labile solid support **2** ensured that each substrate candidate would be

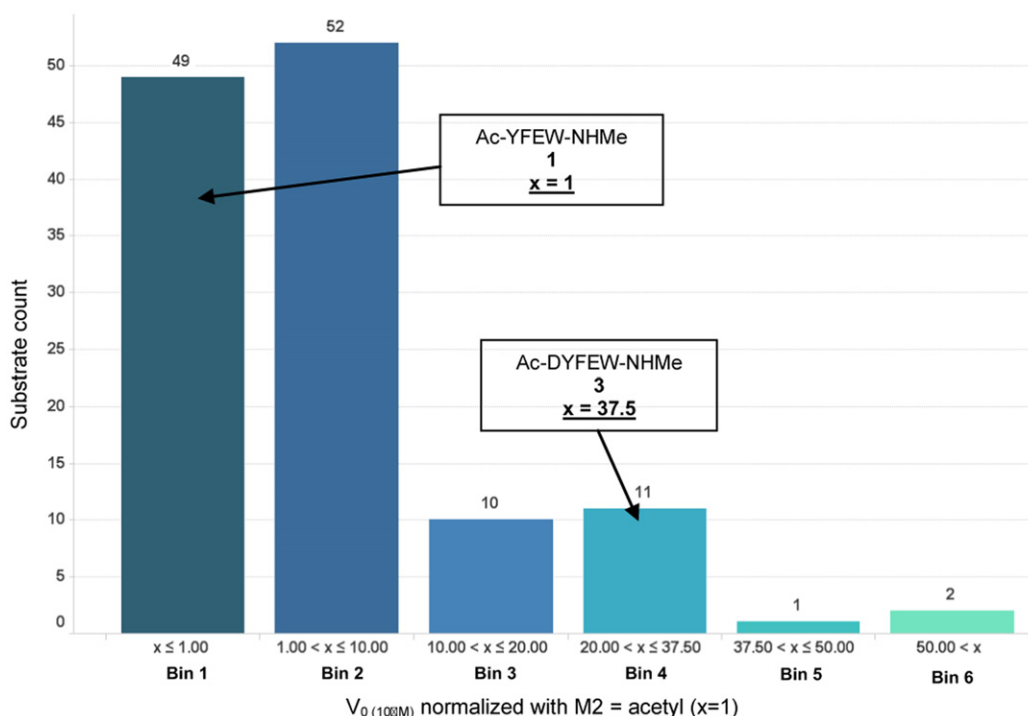
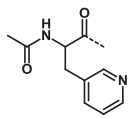
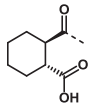
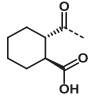
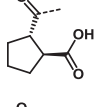
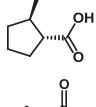
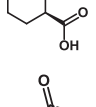
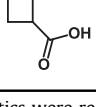


Fig. 5. Primary screen of module 2 building blocks. Substrates have been grouped in bins according to their $V_{0(100M)}$ normalized with M2 = acetyl ($x = 1$).

Table 1
Module 2 optimization: Michaelis–Menten constants for a selection of substrates.

Entry	Module 2	Substrate	K_M (μM) ^a	V_{Max} (nM s^{-1}) ^a	$V_{0\ 10\ \mu\text{M}}$ (nM s^{-1}) ^a	Bin
1	H-	4	No phosphorylation ^b			
2	Ac-	1	232 ± 29	4.4 ± 0.9	0.17 ± 0.07	1
3	Ac-Asp-	3	16.0 ± 4.2	13.7 ± 0.3	6.2 ± 0.1	4
4	Ac-Glu-	5	114 ± 15	27.6 ± 5.7	2.5 ± 0.1	3
5	COOH-(CH ₂) ₂ -	6	144 ± 19	23.3 ± 1.5	1.45 ± 0.4	2
6		7	> 1000 ^c	n.d. ^c	0.4 ± 0.1	1
7		8	204 ± 27	21.7 ± 2.9	1.1 ± 0.1	2
8		9	8.6 ± 1.2	12.8 ± 2.5	10.9 ± 0.1	6
9		10	230 ± 19	24.3 ± 3.3	0.84 ± 0.04	2
10		11	15.1 ± 0.2	11.1 ± 2.2	5.4 ± 0.1	4
11		12	28.7 ± 6.9	16.9 ± 1.1	4.6 ± 0.1	4
12		13	36.9 ± 0.9	13.3 ± 1.1	4.3 ± 0.1	4

^a Kinetics were recorded as 3 independent experiments using the ADP Quest™ assay (See Experimental section).

^b No phosphorylation was detected with substrate concentration up to 1 mM.

^c An accurate value could not be determined due to the limited solubility of the substrate above 1 mM.

released from the resin as the *N*-methyl carboxamide (Scheme 1). In addition, Ac-Asp-OH was added to the diversity set to serve as an internal control for the methodology since we had previously identified the pentapeptide Ac-DYFEW-NHMe **3** (Scheme 1, Module 2 = Ac-Asp-) as a very efficient IGF-1R substrate [7].

Each library member was then subjected to phosphorylation by IGF-1R in our optimized ADP Quest™ assay. Although the determination of K_M values is the method of choice, it would be impractical for larger libraries. As we accepted that our readout sacrifice those substrate candidates for which the phosphorylation reaction was sluggish (either through poor recognition, slow phosphate transfer or slow product dissociation), we chose to classify the library members according to initial phosphorylation velocity at a concentration of 10 μM . We indeed surmised that good substrate recognition would be a prerequisite for fast kinase-catalysed reactions and that this plate-based readout would allow rapid identification of the best candidates.

Gratifyingly, a broad range of substrate behaviour was detected by the assay (Fig. 5). As expected, a majority of modules 2 led to relatively incompetent substrates falling within the “acetyl” bin

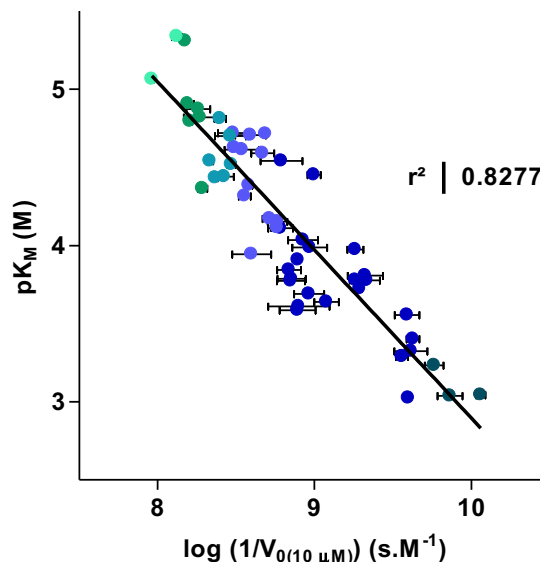


Fig. 6. Correlation between $\log(1/V_{0(10\ \mu\text{M}})$ and pK_M values for a selection of 50 substrates. Dot colour correlates with the bins in Fig. 5. (For interpretation of the references to colour in this figure legend, the reader is referred to the web version of this article.)

and largely derived from purely hydrophobic or positively-charged moieties. A small portion of the library exhibited initial phosphorylation velocities comparable to that of the optimized substrate Ac-DYFEW-NHMe **3** (Table 1, entry 3) with five candidates being phosphorylated at a faster initial rate.

In order to verify our assumption that a correlation could be found between initial velocities at 10 μM and K_M , the Michaelis–Menten constant was recorded for a diverse selection of 50 substrates randomly selected from each bin. A good correlation ($r^2 = 0.82$, Fig. 6) was obtained between pK_M and $\log(1/V_{0(10\ \mu\text{M}})$, thus confirming that the initial rate of phosphorylation was an adequate, easily accessible surrogate readout for substrate efficiency.

The most efficient substrate in the library made use of (*S,S*)-cyclohexyl-1,2-dicarboxylic acid as module 2 (**9**, Table 1, entry 8), affording a 16-fold improvement of substrate **1** (Table 1, entry 2) and a 2-fold improvement of positive-control substrate **3** (Table 1, entry 3) [10]. Interestingly, rigidification of the vector delivering a carboxylate anion to the protein formally allowed for the removal of a hydrogen bond donor–acceptor moiety in the form of the *N*-acetyl group of **3** (Fig. 7). It is worth noting that the enantiomeric module 2 derived from (*R,R*)-cyclohexyl-1,2-dicarboxylic acid led to a very poor substrate of IGF-1R (**8**, Table 1, entry 7). A similar situation was observed in the cyclopentyl series (**9** and **10**, Table 1, entries 9 and 10), providing us with first indications of a responsive SAR for substrates not entirely composed of proteinogenic amino acids.

Having observed dynamic effects on substrate efficiency upon variation of module 2, we turned our attention to alterations of module 1. For this exercise, we decided to keep module 2 constant as *N*-acetyl aspartic acid. We anticipated that tryptophan variations were most likely to give rise to responsive SAR in a proof of concept study, thus making this residue an ideal point of diversity. However, the nature of the solid-phase peptide synthesis used for the elaboration of the substrates imposed that the tryptophan replacement be introduced as the first chemical step on the resin. We envisaged that a fragment coupling strategy would greatly reduce the numbers of individual manipulations necessary for the elaboration of each substrate. It is however well known that fragment coupling

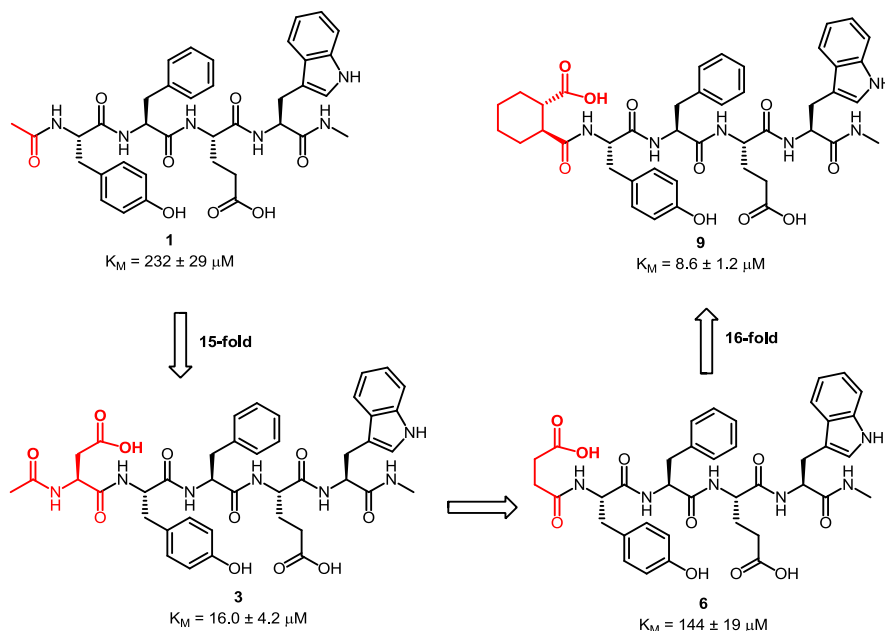


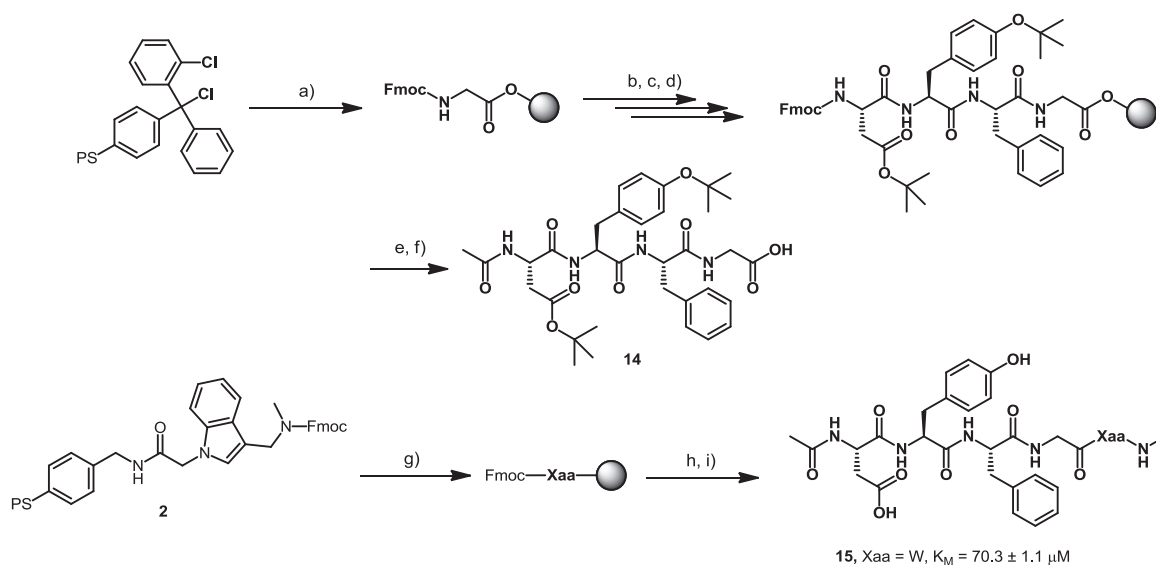
Fig. 7. Structure of the M2-optimized substrate 9.

can lead to racemisation of the fragment's carboxy terminus upon activation. Replacement of the glutamic acid residue in module 1 by glycine would enable a fragment coupling strategy without any risk of racemisation. We therefore synthesized the substrate candidate Ac-DYFGW-NHMe **15** as a new reference substrate (M2: Ac-D; M1: FGW-NHMe).

Satisfactorily, the K_M value of **15** was determined to be $70 \mu\text{M}$, a value well situated in the dynamic range of the ADP Quest™ assay and offering a suitable window for the determination of tryptophan replacement SAR. We decided to limit ourselves to hydrophobic variations, assuming from previous work [7] and known structural information [11] that ablation of the key Van-der-Waals interactions would largely lead to inactive substrates, which would add

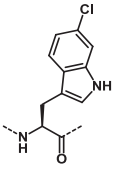
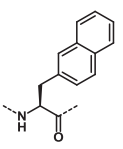
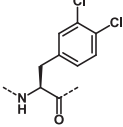
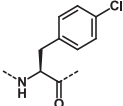
little value to our effort. Thus, a collection of 35 substrates was synthesized according to Scheme 2. The fragment **14** common to all substrate candidates was obtained on large scale by Fmoc/tBu-Boc solid-phase peptide synthesis on (2-chloro)-trityl chloride polystyrene resin. A set of 35 *N*-Fmoc-protected amino acid tryptophan replacements were independently loaded onto resin **2**. Following *N*-Fmoc deprotection, the 35 resins were derivatized with fragment **14**. Subsequent deprotection and cleavage from the support afforded the substrate array.

Phosphorylation rates at $10 \mu\text{M}$ substrate concentration were then recorded [12]. Perhaps not surprisingly, it appeared difficult to improve upon nature's choice of a hydrophobic moiety using essentially the same delivery vector in the form of an amino acid



Scheme 2. Strategy for the synthesis of the M1 library. a) Fmoc-Gly-OH, DIEA, DCM, 2×90 min; b) DMA:Piperidine (4:1), 3×30 min then Fmoc-Phe-OH, HCTU, DIEA, NMP, 90 min; c) DMA:Piperidine (4:1), 3×30 min then Fmoc-Tyr(tBu)-OH, HCTU, DIEA, NMP, 90 min; d) DMA:Piperidine (4:1), 3×30 min then Fmoc-Asp(tBu)-OH, HCTU, DIEA, NMP, 90 min; e) DMA:Piperidine (4:1), 3×30 min then DMA:Ac₂O:pyridine (8:1:1), 90 min; f) DCM:HFIP (4:1), 2×60 min; g) DMA:Piperidine (4:1), 3×30 min then Fmoc-Xaa-OH, HCTU, DIEA, NMP, 2×90 min; h) DMA:Piperidine (4:1), 3×30 min then **14**, HCTU, DIEA, NMP, 2×90 min; i) TFA:TIS:H₂O (95:2.5:2.5), 3×30 min.

Table 2
Module 1 optimization: Replacement of the tryptophan residue on Ac-DYFG-Xaa-NHMe substrates.

Entry	W-replacement	Substrate	K_M (μM) ^a	V_{Max} (nM s^{-1}) ^a	V_0 10 μM (nM s^{-1}) ^a
1	-Trp-	15	70.3 ± 1.1	8.9 ± 0.8	1.7 ± 0.1
2	-D-Trp-	16	907 ± 14	5.2 ± 1.2	0.09 ± 0.01
3		17	19.3 ± 3.7	6.9 ± 0.7	2.1 ± 0.1
4		18	473 ± 21	12.7 ± 2.1	0.24 ± 0.05
5		19	106 ± 9	4.7 ± 1.3	0.55 ± 0.02
6		20	156 ± 21	8.2 ± 1.2	0.47 ± 0.05

^a Kinetics were recorded as 3 independent experiments using the ADP Quest™ assay (See [Experimental section](#)).

side chain. Nevertheless, a handful of candidates actually underwent phosphorylation faster than the tryptophan-containing parent substrate. Among those, the substrate obtained with 6-chlorotryptophan underwent phosphorylation at the fastest rate. Again, we determined the Michaelis–Menten constants of a representative set to check the V_0 – K_M correlation ([Table 2](#)) and confirm

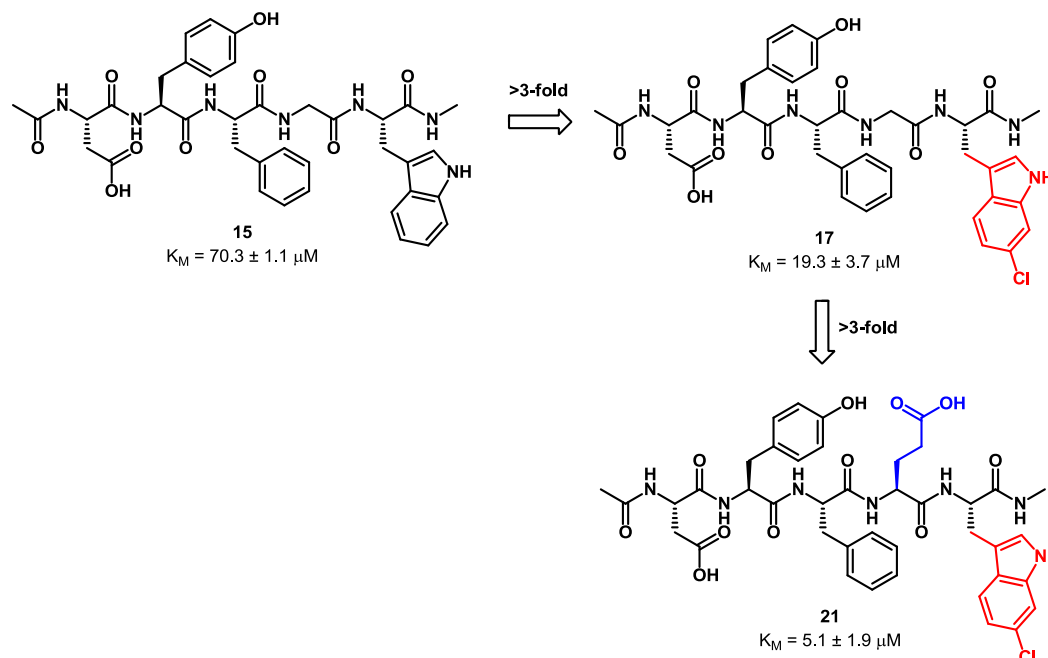


Fig. 8. Structure of the W-optimized substrates **17** and **21**.

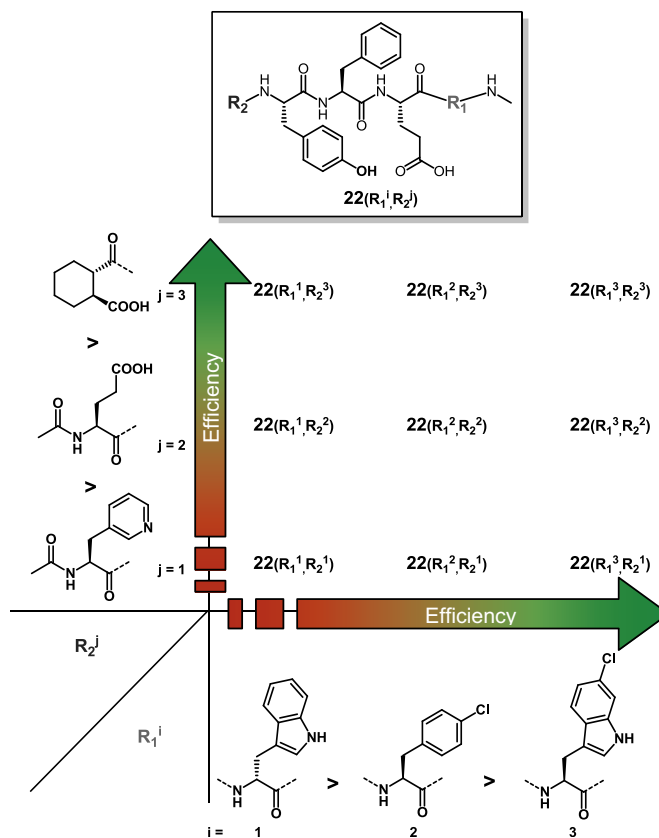


Fig. 9. Selection of the nine combination substrates $22(R_1^i, R_2^j)$.

that 6-Cl-tryptophan substrate **17** was indeed the most efficient one ([Table 2](#), entry 3).

Finally, glutamic acid was re-introduced in place of glycine and, as expected, an improvement of the K_M value was observed across all peptides, with the 6-chlorotryptophan derivative **21** being again the most efficient substrate ([Fig. 8](#)) [13].

Table 3
Michaelis–Menten constants of the M1–M2 combination substrates **22**(R_1^i, R_2^j).

Entry	Substrate	K_M (μM) ^a	V_{Max} (nM s^{-1}) ^a	V_0 $_{10 \mu\text{M}}$ (nM s^{-1}) ^a
1	22 (R_1^3, R_2^3)	<5 μM ^b	11.1 \pm 0.4	7.5 \pm 0.1
2	22 (R_1^3, R_2^2)	23.5 \pm 1.0	10.9 \pm 0.5	3.3 \pm 0.1
3	22 (R_1^3, R_2^1)	35.3 \pm 4.0	5.2 \pm 0.9	1.0 \pm 0.1
4	22 (R_1^2, R_2^3)	15.4 \pm 3.9	9.9 \pm 1.0	4.0 \pm 0.1
5	22 (R_1^2, R_2^2)	278 \pm 72	8.7 \pm 1.8	0.26 \pm 0.04
6	22 (R_1^2, R_2^1)	>1 mM ^c	n.d. ^c	n.d. ^c
7	22 (R_1^1, R_2^3)	188 \pm 18	9.1 \pm 1.9	0.51 \pm 0.01
8	22 (R_1^1, R_2^2)	>1 mM ^c	n.d. ^c	n.d. ^c
9	22 (R_1^1, R_2^1)	>1 mM ^c	n.d. ^c	n.d. ^c

^a Kinetics were recorded as 3 independent experiments using the ADP Quest™ assay (See Experimental section).

^b The lower limit of the assay was reached.

^c An accurate value could not be determined due to the limited solubility of the substrate above 1 mM.

At this stage of the study, we had demonstrated that the rapid initial velocity readout in our simple ADP accumulation assay system was able to provide information on the structure–efficiency relationship around variations of two independent diversity elements. We decided to validate the modular substrate optimisation approach by verifying the additivity of SAR across modules. To this end we combined three modules 1 with three modules 2, making sure to choose moieties having a marked influence on substrate efficiency. Nine combination substrates were synthesized on indole-functionalized resin **2** (Fig. 9). The substrates were submitted to kinase-mediated phosphorylation, and initial velocities at 10 μM as well as Michaelis–Menten parameters were determined (Table 3). We were satisfied to see that the synergy between the two modules was exclusively additive and that, as

a consequence, the combination of the best modules led to the best substrate **22**(R_1^3, R_2^3) in terms of V_0 and K_M . Due to a limitation inherent to the assay format [9], an accurate value for the K_M of **22**(R_1^3, R_2^3) could unfortunately not be precisely determined. Nevertheless, the stage was set for applying the final step of our methodology: the conversion of substrates into inhibitors and the confirmation that substrate SAR translates into inhibitor SAR.

Two tyrosine phosphorylation transition state mimetics have been described in the literature: the hydroxymethyltyrosine phosphate **23** of Hangauer et al. [14] and the meta-iodo-tyrosine **24** used by Lam et al. [15] to convert c-Src kinase substrates into inhibitors (Fig. 10). We decided to use the hydroxymethyltyrosine phosphate derivative **23** to eliminate the risk that residual phosphorylation of meta-iodo-tyrosine complicate assay readouts. A protected version of **23** was synthesized according to published procedures [16], starting from Cbz-Tyr(Tf)-Bzl **26**. The final compound **25** was obtained as a mixture of two diastereoisomers.

The nine substrates **22**(R_1^i, R_2^j) chosen for the SAR additivity study were converted to the corresponding nine inhibitors (Fig. 11, **27**(R_1^i, R_2^j)) by substitution of tyrosine with mimetic **23**. The initial peptide hit **3** was also converted to the corresponding inhibitor **28** ($R_1 = \text{W}, R_2 = \text{Ac-D}$) and served as benchmark. The ability of each inhibitor to impair IGF-1R-mediated phosphorylation of a common generic substrate was then assessed in a standard ATP depletion assay (Table 4) [17]. To our delight, the efficiency trends observed for the substrates translated into comparable inhibitory trends with the most efficient substrate **22**(R_1^3, R_2^3) giving rise to the best inhibitor **27**(R_1^3, R_2^3). This finding was the definite proof that the SAS methodology can be applied to tyrosine kinases and has value as a modular methodology for the generation of substrate-site kinase inhibitors.

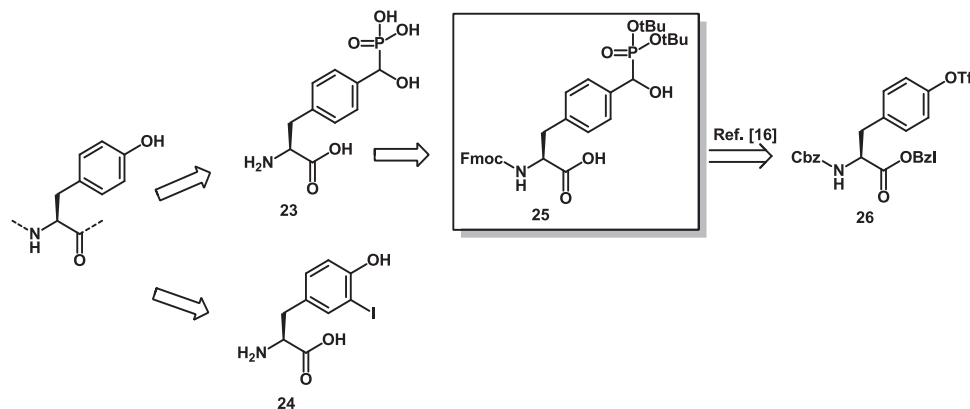


Fig. 10. Tyrosine mimetics described in the literature and the building block **25** used in our synthetic sequence.

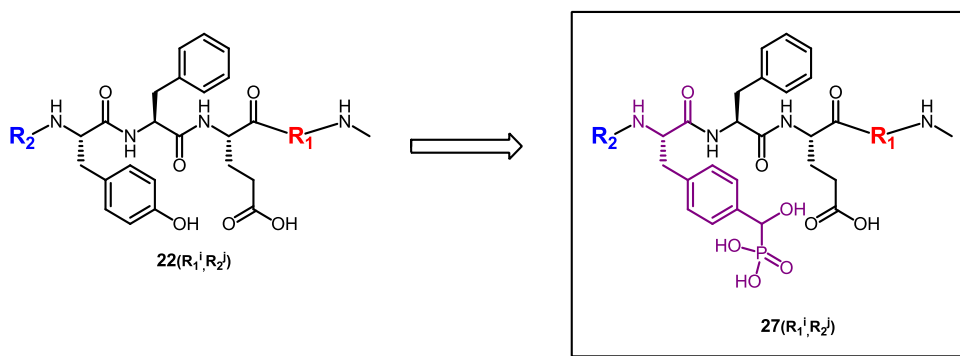


Fig. 11. Inhibitors synthesized for the validation of the SAS methodology.

Table 4
IC₅₀ values of the M1–M2 combination inhibitors **27**(R₁ⁱ, R₂^j).

Entry	Inhibitor	IC ₅₀ (μM) ^a
1	27 (R ₁ ³ , R ₂ ³)	2.5 ± 0.8
2	27 (R ₁ ³ , R ₂ ²)	21.6 ± 6.6
3	27 (R ₁ ³ , R ₂ ¹)	94 ± 29
4	27 (R ₁ ² , R ₂ ³)	14.0 ± 2.5
5	27 (R ₁ ² , R ₂ ²)	40.5 ± 4.6
6	27 (R ₁ ² , R ₂ ¹)	489 ± 29
7	27 (R ₁ ¹ , R ₂ ³)	22.8 ± 5.7
8	27 (R ₁ ¹ , R ₂ ²)	51.3 ± 8.1
9	27 (R ₁ ¹ , R ₂ ¹)	78.2 ± 6.5
10	28	15.6 ± 3.0

^a IC₅₀'s were recorded as 3 independent experiments using KinaseGlo™ assay (See Experimental section).

3. Conclusion

To summarize, we have shown that a substrate of a receptor tyrosine kinase can be optimized in a modular, combinatorial manner. Notably, we have shown that two independent points of diversity can be easily varied to increase substrate efficiency and that the combination of favourable elements led to increased turnover in an additive manner. Finally, we have shown that structure–efficiency relationships of the substrates translated well into structure–activity relationships of the inhibitors upon replacement of the phosphorylation warhead by an inactive mimetic. Having successfully shown, with model peptidogenic compounds, that this methodology has potential in the field of kinase inhibition, we now turn our attention to the generation of large, modular libraries of phenol-containing small-molecules. We are anticipating that these libraries will provide initial, drug-like compounds to feed the optimization methodology. A second research arm in our laboratories aims at identifying new tyrosine mimetics compatible with cell wall permeation, and results will be disclosed in due course.

4. Experimental section

4.1. Chemistry

4.1.1. General remarks

Reagents were used as received and chemicals of the quality *purum*, *purum p. a.* or >98% were used without further purification. All solvents were at least reagent grade. The {3-[(methyl-Fmoc-amino)-methyl]-indol-1-yl}-acetyl AM resin **2** was purchased from EMD Chemicals Inc. Evaporations were carried out under reduced pressure. MS (ESI) were obtained from a Waters SQ Detector and the accurate mass measurements (HR-MS) were performed by using electrospray ionization in positive ion modus after separation by liquid chromatography. The elemental composition was derived from the averaged mass spectra acquired at the high resolution of about 30,000 on an LTQ Orbitrap XL mass spectrometer (Thermo Scientific). The high mass accuracy below 1 ppm was obtained by using a lock mass. NMR spectra's of compounds **14** and **27**(R₁³, R₂³) were recorded on a Bruker spectrometer pulsed at 600 MHz at 298 K in DMSO-*d*₆.

4.1.2. General procedure for the SPPS on the indole-functionalized resin **2**

The peptides and semi-peptidic compounds were synthesized on a Prelude peptide synthesizer (Protein Technologies Inc.) following standard SPPS procedures. The indole-functionalized solid support **2** was swelled in DMA and the Fmoc group removed using three consecutive treatments with 20% piperidine in DMA for 15 min. The resin was washed twice with DMA and then

submitted to two consecutive 30 min treatments with a solution of the first Fmoc-protected amino acid (3 equiv., 0.3 M), HCTU (3 equiv., 0.3 M) and DIEA (4.5 equiv. 0.9 M) in NMP. The resin was washed twice with DMA and capped with a solution of DMA:Ac₂O:pyridine (8:1:1) for 30 min. The resin was finally washed three times with DMA. This protocol was repeated for the loading of each amino acid or M2–COOH. In the case of an amino acid as N-terminus, the resin was acetylated by removing the Fmoc group with 20% piperidine in DMA (three times 15 min) followed by treatment with a solution of DMA:Ac₂O:pyridine (8:1:1) for 30 min. The compound was then released by two consecutive treatment of the beads with a solution of TFA:TIS:H₂O (95:2.5:2.5) for 2 h. The cleavage solutions were then combined and the solvents were removed under reduced pressure. The crude product was then purified by preparative reversed-phase HPLC (Waters, Sunfire™ C₁₈ OBD™ 5 μM, 30 × 100 mm) using gradients of water (+0.1% TFA) and acetonitrile at a flow rate of 30 mL/min and using a DAD UV detector. Product purity was assessed by UPLC on Waters Acquity analytical instruments. The structure of the pure peptidic substrates and inhibitors were confirmed by ESI-MS and by HR-MS spectroscopy. Conditions, instrument specifications and results are listed in the [Supplementary material](#).

Compound stock solutions were then prepared using DMSO:H₂O (75:25).

4.1.3. Synthesis of fully protected fragment **14**

(2-Chloro)-trityl chloride resin (15.2 g, 1 mmol/g) was swelled in DCM and then treated with Fmoc-Gly-OH (9.02 g, 30.3 mmol, 2 equiv.) and DIEA (10.6 mL, 60.7 mmol, 4 equiv.) in DCM (150 mL) for 4 h at 25 °C. The resin was washed twice with DCM:MeOH:DIEA (17:2:1), twice with DCM and twice with DMA. The next amino acids (Fmoc-Phe-OH, Fmoc-Tyr(tBu)-OH and Fmoc-Asp(tBu)-OH) were loaded using classical SPPS procedures: the Fmoc protecting group was removed using 20% piperidine in DMA (150 mL, three times 15 min) and the resin was washed twice with DMA. The resin was then shaken with the Fmoc-protected amino acid (45.6 mmol, 3 equiv.), HCTU (14.6 g, 45.6 mmol, 3 equiv.) and DIEA (11.9 mL, 68.4 mmol, 4.5 equiv.) in NMP (150 mL) for 15 h at rt. The beads were washed twice with DMA and treated with a capping solution made of DMA:Ac₂O:pyridine (8:1:1, 150 mL) for 30 min. The resin was finally washed thrice with DMA. After the last amino acid coupling, the Fmoc group was removed using 20% piperidine in DMA (150 mL, three times 15 min) and the resin was washed twice with DMA. The resin was then shaken with DMA:Ac₂O:pyridine (8:1:1, 150 mL) for 30 min and washed thrice with DMA. The protected fragment was cleaved off the resin by treatment with DCM:hexafluoroisopropanol (4:1, 150 mL, two times 60 min) and the solvents were removed under vacuum. The crude product was purified by reverse phase chromatography on a Büchi Purification System using a gradient of acetonitrile (35–100% in 20 min) in water (+0.1% TFA) at a flow of 50 mL/min to afford **14** (6.36 g) as a white powder after removal of solvents and lyophilization.

Yield: 64%; ¹H NMR (600 MHz, DMSO-*d*₆) δ ppm 13.2–11.9 (brs, 1H, COOH), 8.16 (t, *J* = 5.67 Hz, 1H), 8.04 (dd, *J* = 11.2, 8.6 Hz, 2H), 7.67 (d, *J* = 8.05 Hz, 1H), 7.24–7.21 (m, 4H), 7.18 (m, 1H), 7.03 (d, *J* = 8.42 Hz, 2H), 6.80 (d, *J* = 8.42 Hz, 2H), 4.57–4.50 (m, 2H), 4.43–4.39 (m, 1H), 3.78 (d, *J* = 5.85 Hz, 2H), 3.05 (dd, *J* = 13.9, 4.76 Hz, 1H), 2.89 (dd, *J* = 13.9, 4.39 Hz, 1H), 2.83 (dd, *J* = 13.9, 9.15 Hz, 1H), 2.70 (dd, *J* = 13.9, 9.15 Hz, 1H), 2.53 (dd, *J* = 10.3, 5.49 Hz, 1H), 2.30 (dd, *J* = 15.7, 8.78 Hz, 1H), 1.79 (s, 3H), 1.36 (s, 9H), 1.26 (s, 9H); UPLC (Waters Acquity, UPLC HSS T₃ 1.8 μm, 2.1 × 50 mm, flow rate: 1.2 mL/min, 2 μL injection, 2–98% water (+0.05% HCOOH + 0.05% NH₄OAc) in acetonitrile (+0.05% HCOOH) in 9.4 min, DAD TIC 210–350 nm): *R*_t = 3.75 min, >95% DAD TIC; MS (ESI) 655.4 for [M + H]⁺ (calcd 655.3 for C₃₄H₄₆N₄O₉).

4.1.4. Characterization of fully optimized inhibitor **27**(R_1^3 , R_2^3)

^1H NMR (600 MHz, DMSO- d_6) δ ppm 10.98 (brs, 1H), 8.15 (dd, $J = 12.08, 7.68$ Hz, 1H), 7.93 (d, $J = 6.59$ Hz, 1H), 7.85 (d, $J = 7.68$ Hz, 1H), 7.83–7.78 (m, 2H), 7.56 (d, $J = 8.78$ Hz, 1H), 7.36 (s, 1H), 7.31–7.23 (m, 6H), 7.19 (t, $J = 7.00, 6.95$ Hz, 1H), 7.17 (brs, 1H), 7.09 (d, $J = 7.68$ Hz, 2H), 6.99 (d, $J = 8.42$ Hz, 1H), 4.65 (d, $J = 13.54$ Hz, 1H), 4.51–4.46 (m, 1H), 4.43 (q, $J = 6.95$ Hz, 1H), 4.39–4.33 (m, 1H), 4.30–4.24 (m, 1H), 3.13–3.01 (m, 2H), 2.99–2.88 (m, 3H), 2.74–2.65 (m, 1H), 2.54 (d, $J = 4.02$ Hz, 3H), 2.48–2.42 (m, 1H), 2.42–2.36 (m, 1H), 2.22 (t, $J = 7.87$ Hz, 2H), 2.01–1.95 (m, 1H), 1.84–1.85 (m, 1H), 1.82–1.73 (m, 1H), 1.71–1.55 (m, 3H), 1.29–1.10 (m, 3H), 1.09–0.98 (m, 1H); UPLC (Waters Acquity, UPLC HSS T_3 1.8 μm , 2.1 \times 50 mm, flow rate: 1.2 mL/min, 2 μL injection, 2–98% water (+0.05% HCOOH + 0.05% NH_4OAc) in acetonitrile (+0.05% HCOOH) in 9.4 min, DAD TIC 210 – 350 nm): $R_t = 2.97$ min, >95% DAD TIC; MS (ESI) 939.2 for $[\text{M} + \text{H}]^+$ (calcd 939.3 for $\text{C}_{44}\text{H}_{52}\text{ClN}_6\text{O}_{13}\text{P}$); HR-MS (ESI) 939.30873 for $[\text{M} + \text{H}]^+$ (calcd 939.30917 for $\text{C}_{44}\text{H}_{52}\text{ClN}_6\text{O}_{13}\text{P}$).

4.2. Enzymatic assays

4.2.1. Expression and purification of IGF-1R tyrosine kinase

The cloning, expression and purification of both GST-His₆-tagged kinases was performed as reported previously [18]: Briefly, the cDNA encoding for the entire cytoplasmic domain of human IGF-1R (aa 960–1367) was cloned into the pFastBacGST2-PreScission vector, and a His₆-tag was introduced at the C-terminus of the coding sequences. Proteins were expressed in *Spodoptera frugiperda* Sf9 cells. For the production of unphosphorylated protein, vector encoding for the phosphatase YopH was co-expressed with the IGF-1R vector. The soluble protein obtained from cell lysates was purified by two-step affinity chromatography purification (Glutathione sepharose 4B and His-Trap HP columns). Protein concentration was determined by the Bradford method, and the purity of the protein was determined by SDS-PAGE analysis and HPLC.

4.2.2. Assessment of Michaelis–Menten kinetics with ADP Quest™ assay

IGF-1R kinase was pre-activated as follows: 15 mM HEPES (pH 7.4), 20 mM NaCl, 1 mM EGTA, 0.02% Tween 20, 10 mM MgCl_2 , 0.1 mg/mL BSA, 1850 ng/ μL GST-His₆-IGF-1R and 1.5 mM ATP were incubated for 60 min at 25 °C, then aliquoted and frozen at –80 °C. Kinase reactions were carried out in 384-well plates: 15 mM HEPES (pH 7.4), 20 mM NaCl, 1 mM EGTA, 0.02% Tween 20, 10 mM MgCl_2 , 0.1 mg/mL BSA, 0.4 ng/ μL pre-activated GST-His₆-IGF-1R, peptidic or semi-peptidic substrate at concentration ranging from 1 to 1000 μM and ADP Quest™ detection reagents were mixed together. Reactions were then initiated by the addition of ATP at 60 μM f.c. and relative fluorescence was recorded every 2 min for 60 min on a Victor 2™ plate reader (Perkin–Elmer). Michaelis–Menten constants were directly obtained by using the GraphPad Prism® software. $n = 3$.

For assessment of initial phosphorylation rates at 10 μM substrate concentration $V_{0(10 \mu\text{M})}$, the same protocol was used with peptidic or semi-peptidic substrate at 10 μM f.c.

4.2.3. Assessment of inhibitor IC_{50} 's with KinaseGlo™ assay

IGF-1R kinase was pre-activated as follows: 15 mM HEPES (pH 7.4), 20 mM NaCl, 1 mM EGTA, 0.02% Tween 20, 10 mM MnCl_2 , 0.1 mg/mL BSA, 277 ng/ μL GST-His₆-IGF-1R and 50 μM ATP were incubated for 30 min at 25 °C, then aliquoted and frozen at –80 °C. Kinase reactions were carried out in 384-well plates: 15 mM HEPES (pH 7.4), 20 mM NaCl, 1 mM EGTA, 0.02% Tween 20, 10 mM MnCl_2 , 0.1 mg/mL BSA, 0.5 ng/ μL pre-activated GST-His₆-IGF-1R, 5 μM Ac-EAEDPEGDYFEWLE-NHMe substrate [7] and inhibitor **27**(R_1^i , R_2^j) at concentrations ranging from 250 μM to 114 nM were mixed together. Reactions were then initiated by the addition of ATP at

1 μM f.c. and incubated at 25 °C for 25 min. KinaseGlo™ reagent was added and the reaction was incubated for 30 min at 25 °C. Relative luminescence was recorded on a Victor 2™ plate reader (Perkin–Elmer). IC_{50} values were directly obtained by using the GraphPad Prism® software. $n = 3$.

Acknowledgements

We thank Novartis Pharma AG and the Program Office for funding this research, Dr. Patrick Chène, Dr. Philipp Grosche, Stephanie Pickett, Lionel Muller, Nicole Martin and Daniela Manfrina for their collaboration and contribution to this project. We are also grateful to Dr. Christian Guénat, Dr. Ingo Muckenschnabel and Régis Denay for analytical support.

Appendix A. Supplementary data

Supplementary data related to this article can be found at <http://dx.doi.org/10.1016/j.ejmech.2012.08.038>.

References

- [1] P. Cohen, Nat. Rev. Drug Disc 1 (2002) 309–315.
- [2] (a) S.P. Davies, H. Reddy, M. Caivano, P. Cohen, Biochem. J. 351 (2000) 95–105; (b) J. Bain, H. McLauchlan, M. Elliott, P. Cohen, Biochem. J. 371 (2003) 199–204.
- [3] For a review on allosteric inhibitors see R.M. Eglén, T. Reisine, Expert Opin. Drug Discov. 5 (2010) 277–290.
- [4] (a) S.M. Sebt, Q. Cheng, A.D. Hamilton, K. Kayser-Bricker US2010/0009397 A1 (2010). (b) Litman, et al., Biochemistry 46 (2007) 4716–4724; (c) Steiner, et al., Eur. J. Pharm. 562 (2007) 1–11.
- [5] G. Ye, R. Tiwari, K. Parang, Curr. Opin. Invest. Drugs 9 (2008) 605–613.
- [6] M.B. Soellner, K.A. Rawls, C. Grundner, T. Alber, J.A. Ellman, J. Am. Chem. Soc. 129 (2007) 9613–9615.
- [7] J. Chapelat, F. Berst, A.L. Marzinzik, H. Moebitz, P. Drueckes, J. Trappe, D. Seebach, Bioorg. Med. Chem. Lett. 21 (2011) 7030–7033.
- [8] N.W. Charter, L. Kauffman, R. Singh, R.M. Eglén, J. Biomol. Screen. 11 (2006) 390–399.
- [9] The assay system is based on the detection of ADP formed during the course of the phosphorylation reaction and the lowest ADP concentration required for detection is 500 nM. This implied that the minimal substrate concentration still enabling accurate measurements while maintaining low substrate conversion (<20%) was situated around 2.5 μM .
- [10] The K_M value measured for substrate 9 approached the technical limit of 2.5 μM imposed by the ADP-Quest™ assay (see refs. [8,9]), which would hinder any further optimization of module 2. Although we did not want to increase the efficiency at this point in time in our peptide-based proof-of-concept study, we recognized that this limitation might prove problematic when the technology is transferred to small molecule chemical space. We therefore decided to artificially raise the K_M of the substrate by alteration of module 1. This was expected to serve the dual purpose of increasing the dynamic range of the assay, should this be necessary, and of ascertaining that modification of both modules lead to additive SAR. We had previously determined that the tryptophan residue in substrate 3 was key for recognition by IGF-1R. We therefore chose ten substrates from the 125-membered library covering a wide range of K_M values, synthesized the tryptophan-to-phenylalanine mutants and determined their Michaelis–Menten constants. The values are available in the Supplementary material. As anticipated, given the relatively linear conformation required for kinase-mediated peptide phosphorylation, we observed that the K_M values were uniformly shifted towards less efficient substrates upon substitution of the tryptophan residue by phenylalanine.
- [11] The importance of the tryptophan residue and its interaction with the kinase was based on IGF-1R crystal structure PDB ID 1k3a.
- [12] For details see the Supplementary material.
- [13] In order to verify the additivity of the SAR observed with glycine, a set of 6 Trp-modified substrates was synthesized with glutamic acid and the Michaelis–Menten kinetics were measured and compared with the corresponding glycine substrates. The results are available in the Supplementary material.
- [14] M.H. Kim, J.H. Lai, D.G. Hangauer, Int. J. Pept. Protein Res. 44 (1994) 457–465.
- [15] J. Alfaro-Lopez, W. Yuan, B.C. Phan, J. Kamath, Q. Lou, K.S. Lam, V.J. Hruby, J. Med. Chem. 41 (1998) 2252–2260.
- [16] Z.-J. Yao, Y. Gao, T.R. Burke Jr., Tetrahedron: Asymmetry 10 (1999) 3727–3734 (The detailed synthetic sequence is described in the Supplementary material).
- [17] The KinaseGlo™ assay from Promega Corp. was used to determine the IC_{50} 's of IGF-1R inhibitors. For detailed procedure the Supplementary material.
- [18] D. Erdmann, C. Zimmermann, P. Fontana, J.-C. Hau, A. De Pover, P. Chène, J. Biomol. Technol. 21 (2010) 9–17.